Vol. 38 (2007) ACTA PHYSICA POLONICA B No 4

STRUCTURE OF THE $N \sim Z$ $1f_{7/2}$ SHELL NUCLEI*

Călin A. Ur

INFN, Sezione di Padova, 35131 Padova, Italy
and
NIPNE–HH, 077125 Măgurele-Ilfov, România

(Received December 3, 2006)

Detailed experimental investigation with large γ-ray arrays have recently extended the knowledge of many nuclei filling the $1f_{7/2}$-shell nuclei. It was shown that these nuclei are characterized by a large variety of phenomena that originate in their particular location in a mass region between light and heavy nuclei having still a low number of valence particles to allow for full shell model description but already large enough to develop collective behavior with all its consequences. The evolution of their structure with spin and excitation energy is marked by the interplay between the single particle and collective degrees of freedom. Nuclei with $N \sim Z$ are of special interest as they provide valuable information on the proton–neutron interaction and the interplay between the $T = 0$ and $T = 1$ pairing modes. Isospin symmetry studies in $T_z = \pm 1/2$ mirror nuclei and $T_z = 0, \pm 1$ isospin multiplets were facilitated by the experimental identification of states in many of the nuclei filling the $1f_{7/2}$-shell allowing for a systematic study on the origin of the charge symmetry breaking effects. The comparison with accurate large scale shell model calculations leads towards a quantitative understanding of the various contributions to these effects. To illustrate some of the properties that make so appealing these nuclei I discuss in the present paper the $N = Z$ nucleus ^{52}Fe and the $A = 54$ $T = 1$ multiplet.

PACS numbers: 21.10.–k, 21.60.Cs, 23.20.Lv, 27.40.+z

1. Introduction

Generally by $1f_{7/2}$-shell nuclei we identify the region of the nuclide chart with proton and neutron numbers comprised between 20 and 28. These nuclei are described as having a $N = Z = 20$ (^{40}Ca) core while valence particles occupy the pf-shell orbitals. Non-natural parity structures identified

* Presented at the Zakopane Conference on Nuclear Physics, September 4–10, 2006, Zakopane, Poland.

in these nuclei imply the need to consider also particle–hole excitations from the sd-shell into the pf-shell. The mixing of the $f_{7/2}$ and $p_{3/2}$ orbitals is the key feature in these nuclei as it leads to $\Delta j = \Delta l = 2$ quadrupole type correlations that eventually result in large quadrupole deformation and collective behavior [1]. The nuclei in this mass region have still a low enough number of valence particle to allow for full spherical shell model calculations but already high enough to give rise to collective phenomena with all their consequences. For this reason they represent the best ground for comparing very different nuclear models as the shell model and the mean field calculations in the intrinsic reference system providing complementary information on the evolution of their structure. Modern large scale spherical shell model calculations can account in a natural way for the large deformation observed in these nuclei [2] (and references therein). The calculations presented throughout the paper were performed with the code ANTOINE [3].

The experimental knowledge of the $1f_{7/2}$ shell nuclei experienced an explosive expansion during the last decade due to the development of the experimental techniques and instruments for γ-ray and particle spectroscopy. In several nuclei excited states were identified for the first time while in many others, already known from previous studies, the structure was largely extended to high spins and excitation energy. The experimental results evidenced the large variety of phenomena characterizing the nuclei filling the $1f_{7/2}$ shell. They can be summarized as follows: large deformation in the ground state around the middle of the $1f_{7/2}$ shell (the most deformed nucleus is ^{48}Cr [4] with 4 valence protons and 4 valence neutrons); occurrence of rotational bands built on deformed states; single particle and collective behaviors compete to stabilize the structure of these nuclei and the bands often end with band termination where all nucleon pairs are broken; formation of long lived yrast trap states at the band termination (^{52}Fe [5,6]); along the bands back-bending phenomena were identified as due to band crossings (^{50}Cr [7,8]) or termination in seniority subspaces [9]; intruder bands of non-natural parity were identified in many nuclei and they were explained as due to particle–hole excitation from the sd shell into the $f_{7/2}$ shell.

The $N = Z$ and mirror nuclei from this region were populated with relatively high cross section in heavy ion induced fusion–evaporation reactions and they could be studied in detailed up to high spins. Several interesting features emerged from their investigation as: competition between $T = 0$ and $T = 1$ structures in odd–odd $N = Z$ nuclei (^{46}V [10], ^{50}Mn [11]); evolution of the mirror energy difference with spin (^{50}Fe–^{50}Cr [12]); isospin symmetry breaking effects (^{54}Ni–^{54}Co–^{54}Fe [13]).

In the paper I will discuss the structure of the $N = Z$ ^{52}Fe nucleus and the measurement for the first time of the E4 γ-ray decay of the yrast trap at 12^+. I will also present the identification of excited states in the $N = Z-2$

nucleus ^{54}Ni with the γ-ray array EUROBALL and I will comment on the possible interpretation of the mirror energy difference (MED) observed in the $A = 54$ $T = 1$ multiplet.

2. The 12^+ yrast trap in ^{52}Fe and its γ-ray decay

Early β-decay studies established that the yrast 12^+ state of ^{52}Fe [5,14] is a long-lived state with a half-life of 45.9 ± 0.6 sec. From the end-point of the β^+-decay the excitation energy of the state was estimated to be 6820 ± 130 keV. The 12^+ isomer decays primarily by Gammov–Teller transitions towards excited states in ^{52}Mn and an upper limit of 0.4% was established [5] for its γ-ray decay.

More recently, in an experiment performed with the GaSp γ-ray array [6] high spin states in the ^{52}Fe nucleus were populated using the ^{28}Si+^{28}Si fusion–evaporation reaction. States were populated up to spin $10\hbar$ and it confirmed the hypothesis on the location of the long-lived yrast trap at spin $12\hbar$ below the yrast $10\hbar$ state. However, no information on the γ-ray decay of the isomer could be obtained from this measurement.

A dedicated measurement was performed at the GSI on-line mass separator to identify the E4 γ-ray decay of the 12^+ isomer [15]. Population of the yrast 12^+ state in ^{52}Fe was achieved by bombarding a thick ^{28}Si target with a 170 MeV ^{36}Ar beam provided by the UNILAC accelerator. The recoils were stopped in a FEBIAD-E ion source and ionized. After extraction they were mass separated ($A = 52$) and implanted on a tape that each 80 sec. was moved away from the measuring point to eliminate the background due to undesired long-lived activity. Beta detection was performed with a plastic scintillator of $\sim$ 85% efficiency (measured with ^{24}Na source). Gamma rays were detected with a system built of a Cluster detector, a Clover detector and a 60% Ge detector with a total photopeak efficiency of 3.9% at 1.33 MeV. The segmentation of the Ge detectors was essential for keeping the summing effects below the experimental uncertainties. The experiment revealed two gamma rays corresponding to the E4 decay of the 12^+ isomer to the two 8^+ states previously identified [6].

The spectrum presented in Fig. 1 is obtained from a γ–γ coincidence matrix built with a veto condition on the beta counter and by summing the gates on the lowest three transitions in ^{52}Fe. It shows clearly the gamma peaks corresponding to the two E4 γ-ray transitions.

The new data have significantly improved the accuracy on the excitation energy of the 12^+ isomer that is now 6957.4(4) keV. The level scheme of ^{52}Fe with the newly measured E4 transitions is shown in Fig. 2. The figure also shows the β^+-decay pattern towards excited states in ^{52}Mn as observed in the measurement.

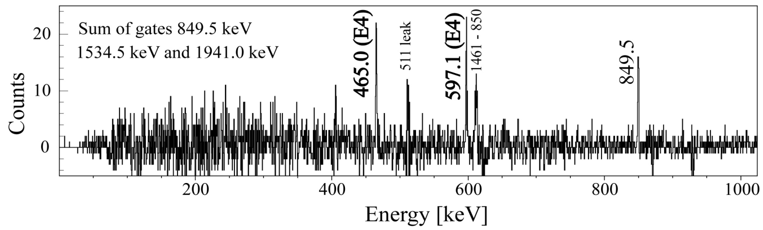

Fig. 1. Gamma coincidence spectrum obtained by setting gates on three γ-ray transitions in ^{52}Fe. The spectrum was obtained in anti-coincidence with the beta counter to lower the gamma background due to β-delayed γ-ray transitions. The gamma peaks corresponding to the two E4 transitions from the 12^+ isomer are indicated on the figure with the label E4.

Based on the observed intensities of the E4 transitions very low values of the B(E4) reduced transition probabilities were deduced: $4.6(17) \times 10^{-4}$ W.u. for the 597 keV transition and $3.5(13) \times 10^{-3}$ W.u. for the 465 keV

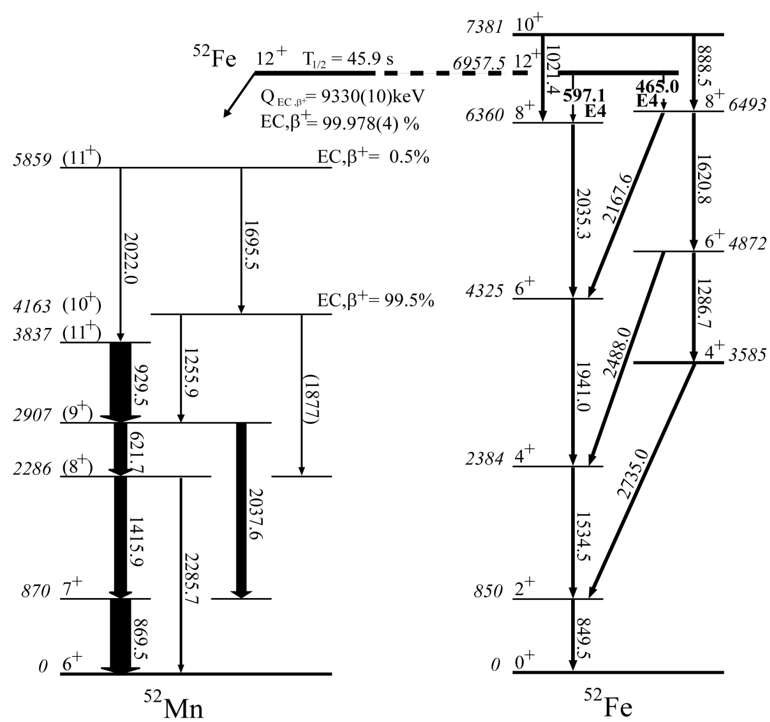

Fig. 2. Level scheme of ^{52}Fe as established from the previous measurement with the GaSp array [6] and the GSI data. The β^+-decay towards excited states in ^{52}Mn is also shown.

transition. These values are the lowest measured in this mass region and explain why these transitions were not observed before [5]. Large scale shell model calculations in the full pf shell were performed with the code ANTOINE [3] and using three different residual interactions: FPD6 [16], KB3G [17] and GXPF1 [18]. The hindrance of the B(E4) values can be understood in terms of the hexadecapole strength distribution. Calculation of the E4 strength from the 12^+ isomer to the all 8^+ states in the pf shell model space indicate that most of the E4 strength is located at excitation energies above the 12^+ state. In fact, calculations show that only 10% for KB3G, 2% for GXPF1 and 0.2% for FPD6, of the E4 strength feed the lowest two 8^+ states.

The experimental positive parity levels of ^{52}Fe are compared with calculations performed with large scale shell model using the KB3G residual interaction, in Fig. 3. Calculations were performed using a $s = 3$ truncation scheme (see Ref. [9] for details). A good agreement between experimental data and calculations is attained.

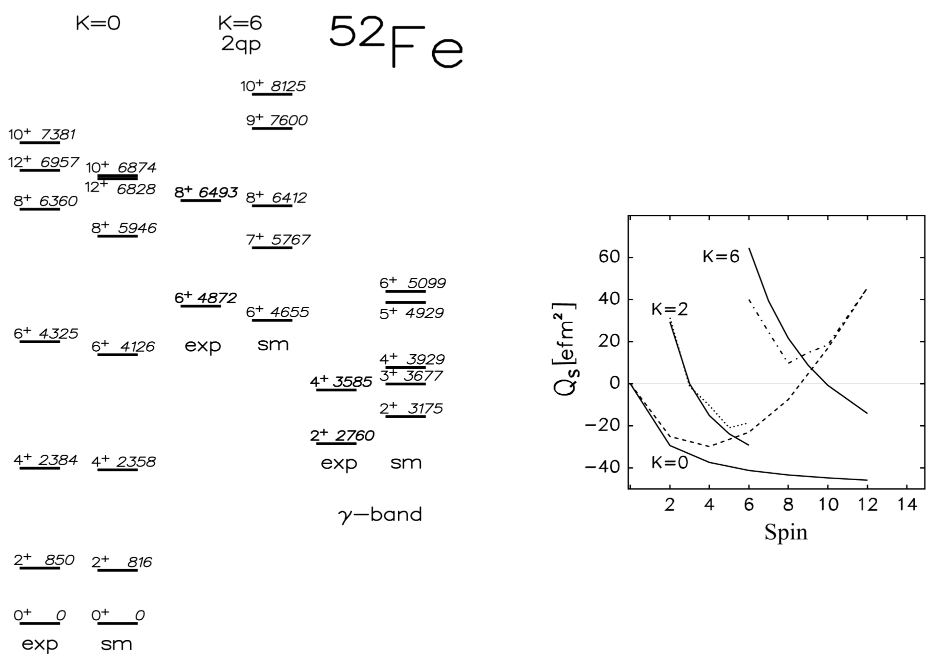

Fig. 3. Shell model calculated states in ^{52}Fe are compared with the experimental level scheme. A general good agreement is observed. The states were organized in bands labeled with the dominant K quantum number. In the right side panel shell model spectroscopic quadrupole moments (dotted and dashed lines) are compared with the predictions of the rotor model (full lines) for a deformation parameter $\beta = 0.24$.

It was discussed in Ref. [9] that low-lying states in the $1f_{7/2}$-shell nuclei can be classified in the framework of the Nilsson diagram and the K quantum number can be successfully used for labeling the different band structures. In ^{52}Fe the presence of the second 6^+ and 8^+ excited states is associated with a $K = 6$ two quasiparticle band originating from the excitation of one proton or one neutron from the $[312]5/2^-$ orbital to the $[303]7/2^-$ orbital. The band labeled with $K = 2$ is a good candidate for the γ-band; the structure of the states in this band appear to have a very fragmented wavefunctions while for the other bands with $K = 0$ (ground state band) and $K = 6$ the structure of the states is dominated by the $(f_{7/2})^{12}$ configuration.

The shell model calculated spectroscopic quadrupole moments shown in Fig. 3 depart from the rotor prediction above spin $4\hbar$ cross the zero line at spin around $10\hbar$ and end with a large positive value for the 12^+ state. There might be two explanation of this large positive value for the 12^+ state: (a) the yrast 12^+ state is a four quasiparticle $K = 12$ state corresponding to the simultaneous excitation of one neutron and one proton from the $[312]5/2^-$ orbital to the $[303]7/2^-$ orbital or (b) the yrast 12^+ state corresponds to a non-collective prolate shape. Shell model calculations [9] and experimental lack of evidence for a band structure built on the supposed $K = 12$ band head favor the second hypothesis case in which the yrast 12^+ state is a real band termination in the $(f_{7/2})^{12}$ configuration space.

3. Identification of the $N = Z - 2$ ^{54}Ni nucleus

The charge invariance of the nucleon–nucleon force leads to the isospin symmetry. This symmetry is broken by the electromagnetic forces and to a lesser extent by the strong interaction with the result that isospin is not exactly a good quantum number. This means that nuclear states are expected to contain, besides the main component of isospin, also small components of different isospin. The degree of isospin mixing is a measure of the symmetry violation. Measuring the strength of forbidden E1 γ-ray transitions in $N = Z$ nuclei can be an effective way to estimate isospin mixing [19]. In mirror nuclei the information is provided by the difference between analog E1 transition strengths. The nuclear contribution to the isospin non-conservation can be extracted from Coulomb energy difference in mirror nuclei (MED) and isospin multiplets (TED). Several mirror nuclei and $T = 1$ multiplets were identified in the $f_{7/2}$ shell giving the opportunity to uncover the microscopic origin of the isospin symmetry breaking terms in the nuclear interactions.

Identification of excited states in the nucleus ^{54}Ni [13] allowed for the study of the Coulomb energy difference within the $A = 54$ $T = 1$ multiplet (^{54}Ni, ^{54}Co, ^{54}Fe). The ^{54}Ni nucleus was populated via the ^{24}Mg(^{32}S,$2n$) reaction at 75 MeV beam energy. The beam was provided by the VIVIT-

RON accelerator at IReS Strasbourg. Gamma rays were detected with the EUROBALL IV γ-ray array composed of 26 Clover and 15 Cluster composite Compton-suppressed Ge detectors, light charged particles with the EUCLIDES Si ball [20] and neutrons with the Neutron Wall [21].

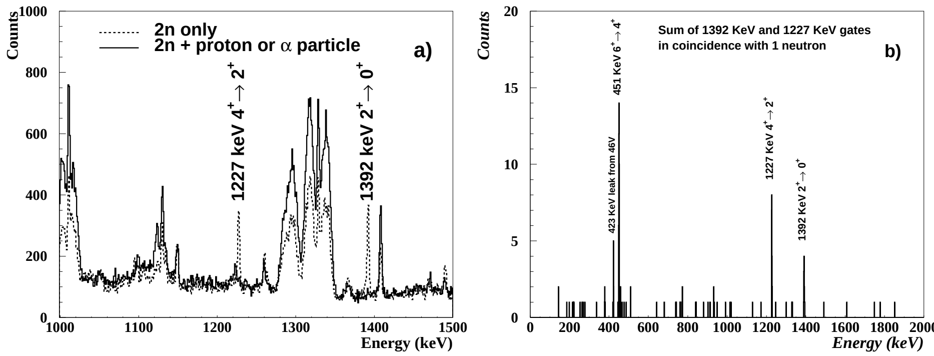

Fig. 4. Assignment of gamma rays to ^{54}Ni was done on the basis of their coincidence or anti-coincidence with charged particles and neutrons. Panel (a) shows two γ-ray spectra: one in coincidence with 2 neutrons and no charged particles (dashed line) and another one in coincidence with 2 neutrons and any charged particle (full line); one can clearly identify the two gamma lines at 1227 keV and 1392 keV that were assigned to ^{54}Ni ($2n$ channel). Panel (b) shows a gated γ-ray spectrum where all three gamma lines assigned to ^{54}Ni are evident.

Gamma rays were assigned to the ^{54}Ni nucleus based on the comparison between the γ-ray spectrum built in coincidence with 2 neutrons and in anticoincidence with charged particles and the γ-ray spectrum conditioned with 2 neutrons and any charged particle. This is illustrated in Fig. 4(a) where two gamma rays assigned to ^{54}Ni are clearly identified. A carefull analysis of all possible sources of contamination in the target was done and it could be concluded with high confidence that the three γ-ray lines of 1392, 1227 and 451 keV belong to ^{54}Ni.

Placement of the gamma rays in the level scheme was done based on the γ–γ coincidence relationships, their relative intensities and from the comparison with the level scheme of the mirror nucleus ^{54}Fe [22]. Gamma rays were assigned an E2 character based on the asymmetry of their intensity distribution as detected in the Cluster detectors (backward direction) and in the Clover detectors (at $\sim 90°$). Therefore the level scheme of ^{54}Ni was established up to spin 6^+ as shown in Fig. 5 (left side).

In Ref. [23] is shown that nuclear isospin symmetry breaking effects (NIB) are as important as those due to the Coulomb potential. The study was carried out for the $A = 42$ isobars and it assumed that the structure of the yrast bands in these nuclei is dominated by the $f^2_{7/2}$ configuration.

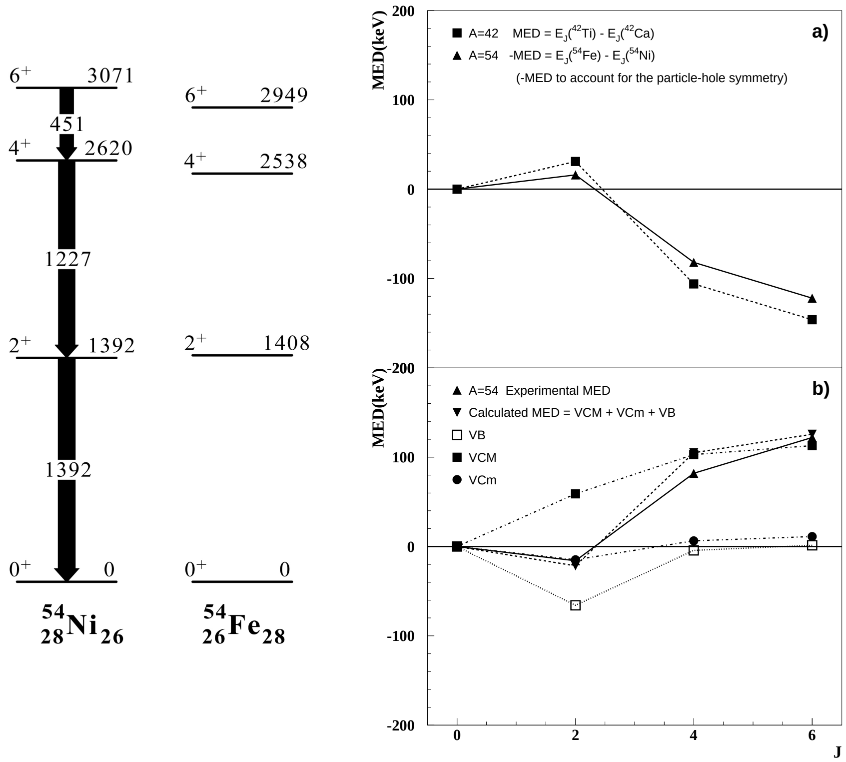

Fig. 5. Level scheme of ^{54}Ni presented together with the relevant part of the level scheme of the mirror nucleus ^{54}Fe. Panel (a) shows the experimental MED values for the $A = 42$ and $A = 54$ mirror nuclei. Shell model calculations are compared with the experimental results in panel (b). The different contributions to the MED values are plotted separately (see text for details).

The difference between the observed and Coulomb-calculated spectra was attributed to NIB effects. It was derived a single term parametrization in terms of $J = 0$ and $J = 2$ pairing operators for TED and MED, respectively, that reproduces well the experimental data available for other mirror nuclei and isobar multiplets in the region. In the $f^n_{7/2}$ configuration space the 2 particle $A = 42$ and the 2 hole $A = 54$ spectra have to be the same, and experimentally they are found to be identical within 150 keV. The experimental MED values were calculated as $\mathrm{MED}_J(A = 54) = E^*_J(^{54}\mathrm{Ni}) - E^*_J(^{54}\mathrm{Fe})$ and $-\mathrm{MED}_J(A = 42) = E^*_J(^{42}\mathrm{Ca}) - E^*_J(^{42}\mathrm{Ti})$. In Fig. 5(a) the MED$(A = 42)$ and MED$(A = 54)$ values are presented as a function of spin. The similarity between the two MED curves is very intriguing. One had to understand why the cross conjugate symmetry in the $f_{7/2}$ shell works so well when it is known that nuclei with $A = 42$ contain strong core excitation in the structure of the lowest excited states and the states in the $A = 54$ nuclei are strongly mixed with the other orbitals of the pf shell. To understand the origin of this similarity large scale shell model calculations in the full pf shell were performed using the KB3G residual interaction. The various contributions to the MED($A = 54$) values as a function of spin were estimated individually and they are shown in Fig. 5(b). The meaning of the different terms is the following: $V_{\rm CM}$ is the Coulomb interaction in the pf shell, $V_{B(1)}$ is the isovector quadrupole pairing NIB, V_{Cm} is the difference in Coulomb repulsion due to the charge radii, C_{ll} and C_{ls} are single-particle contributions of electromagnetic origin. It is evident that the overall behavior of the MED curve is given by the V_{CM} and $V_{B(1)}$ terms while the other terms (V_{Cm}, C_{ll} and C_{ls}) that contain the dependence on the occupancy of the orbitals contribute only a small quantity. This means that the occupancy of the orbitals must be quite independent of J. For all the states involved in the analysis the configuration $f_{7/2}^{14}$ contributes only 60% to the wavefunction. The rest is fragmented among the other orbitals of the pf shell but with weights independent of J. One might conclude that the cross conjugate symmetry breaking terms are not vanishing but they are independent of J and they cancel out in the MED values. This explains why the pure $f_{7/2}$ description works well for the calculating MED values and the similarity between the values for $A = 42$ and $A = 54$.

4. Conclusions

The region of the $1f_{7/2}$-shell nuclei emerge from the nuclear landscape through the richness and large variety of the nuclear phenomena characterizing these nuclei. In the present paper I focused on two recently investigated topics. First, I discussed the γ-ray decay of the 12^+ isomer in the $N = Z$ ^{52}Fe nucleus. Identification of the two strongly hindered E4 γ-ray transitions and comparison of the estimated $B(E4)$ values with state of the art shell model calculations provided the means to distinguish the more realistic wavefunction from those predicted by different effective interactions. Some hints were given to understand the nature of the 12^+ state as prolate non-collective band termination or as a high K prolate deformed band head. Identification of states in the $N = Z - 2$ ^{54}Ni nucleus allowed for the analysis of the mirror energy difference in the $A = 54$ nuclei. A discussion on the cross conjugate symmetry in the $1f_{7/2}$ shell was possible from the comparison with the $A = 42$ mirror nuclei.

The author would like to thank A. Gadea and F. Brandolini for helpful discussions and for the permission to present results prior to their publication.

REFERENCES

[1] E. Caurier *et al., Phys. Rev.* **C50**, 225 (1994).

[2] E. Caurier *et al., Rev. Mod. Phys.* **77**, 427 (2005).

[3] E. Caurier, Code ANTOINE, Strasbourg, 1989; E. Caurier, F. Nowacki, *Acta Phys. Pol. B* **30**, 705 (1999).

[4] S. Lenzi *et al., Z. Phys.* **A354**, 117 (1996).

[5] D.F. Geesaman *et al., Phys. Rev.* **C19**, 1938 (1979).

[6] C.A. Ur *et al., Phys. Rev.* **C58**, 3163 (1998).

[7] S. Lenzi *et al., Phys. Rev.* **C56**, 1313 (1997).

[8] F. Brandolini *et al., Nucl. Phys.* **A642**, 387 (1998).

[9] F. Brandolini, C.A. Ur, *Phys. Rev.* **C71**, 054316 (2005).

[10] S. Lenzi *et al., Phys. Rev.* **C60**, 021303 (1999).

[11] C.E. Svensson *et al., Phys. Rev.* **C58**, 2621 (1998).

[12] S. Lenzi *et al., Phys. Rev. Lett.* **87**, 122501 (2001).

[13] A. Gadea *et al., Phys. Rev. Lett.* **97**, 152501 (2006).

[14] D.F. Geesaman *et al., Phys. Rev. Lett.* **34**, 326 (1975).

[15] A. Gadea *et al., Phys. Lett.* **B619**, 88 (2005).

[16] W.A. Richter *et al., Nucl. Phys.* **A523**, 325 (1991).

[17] A. Poves, E. Caurier, F. Nowacki, *Nucl. Phys.* **A694**, 157 (2001).

[18] M. Honma, *et al., Phys. Rev.* **C65**, 061301 (2002).

[19] E. Farnea *et al., Phys. Lett.* **B551**, 56 (2003).

[20] A. Gadea *et al.*, LNL Annual Report 1996, p. 151, p. 225.

[21] J. Ljungvall, M. Palacz, J. Nyberg, *Nucl. Instrum. Methods*, **A528**, 741 (2004).

[22] D. Rudolph *et al., Eur. Phys. J.* **A4**, 115, (1999).

[23] A.P. Zuker *et al., Phys. Rev. Lett.* **89**, 142502, (2002).